PIER M

*(Received 30 April 2026, Accepted 29 May 2026, Scheduled 18 June 2026)*

# High-Accuracy Dual-Split-Ring-Resonator Microwave Sensor for Permittivity Characterization and Defect Detection in Solid Materials

Tata Setiawan[1], Syah Alam[1,*], Indra Surjati[1], Lydia Sari[1], Yuli K. Ningsih[1], Teguh Firmansyah[2], Yohanes G. Adhiyoga[3], Juliano Katrib[4], and Zahriladha Zakaria[5]

[1]*Graduate programe of Electrical Engineering, Universitas Trisakti, West Jakarta 11440, Indonesia*
[2]*Department of Electrical Engineering, Universitas Sultan Ageng Tirtayasa, Banten 42124, Indonesia*
[3]*Research Centre for Telecommunication, National Research and Innovation Agency (BRIN), Bandung 40135, Indonesia*
[4]*Department of Electrical and Computer Engineering, Gulf University for Science and Technology, 32093, Kuwait*
[5]*Faculty of Electronic and Computer Engineering Technology (FTKEK), Universiti Teknikal Malaysia Melaka (UTeM) 76100 Durian Tunggal, Melaka, Malaysia*

**ABSTRACT:** This research proposes a microwave sensor based on a dual-split-ring-resonator (DSRR) structure designed for the detection of the permittivity of solid samples and defective materials. The DSRR structure was chosen because it has a high-quality factor Q, is highly sensitive to changes in permittivity, and is easy to integrate into a planar substrate. The designed sensor is fabricated using a Rogers RO5880 substrate having a dielectric constant $\varepsilon_r$ of 2.2, $\tan\delta$ of 0.0009, and a substrate thickness $h$ of 1.58; the sensor operates in the frequency range of 1 GHz–2 GHz and adopts a dual-port configuration by observing changes in the transmission parameter $S_{21}$. The measurements used the perturbation theory method, where the resonance frequency shift occurs when a material is inserted into the sensor area. This sensor area is defined as the location of maximum electric-field concentration within the resonator. Polynomial equations are derived for measurements on dielectric materials with known permittivity values ranging from 1 to 9.8. The proposed sensor demonstrates high performance, with a measured accuracy of 99.6%, a normalized sensitivity of 2.6%, and a frequency detection resolution (FDR) of 0.026 GHz. These results indicate that the sensor using the DSRR method with hole integration offers reliable and precise permittivity detection, particularly for detecting defects in materials.

## 1. INTRODUCTION

The development of communication technology and microwave-based detection systems has encouraged the development of various efficient, fast, and accurate nondestructive testing (NDT) measurement methods. Microstrip resonator sensors are an emerging technology that can detect changes in the dielectric properties of materials by altering the electromagnetic field around the resonator [18]. A sensor is a device that can convert physical quantities into electrical signals that can be measured and analyzed [13]. Microwave sensors can detect, measure, and respond to physical or chemical changes in their surroundings, such as temperature, pressure, humidity, and the electromagnetic properties of a material [17]. Microwave sensors can detect changes in the electromagnetic parameters of a material, such as its permeability and permittivity, by utilizing the interaction between the material and electromagnetic waves [10].

Split-ring resonator (SRR) and its derivatives, such as dual-split-ring resonator (DSRR), are among the most commonly used resonator structures for fabricating microwave sensors. A DSRR structure consists of two concentric conducting rings with a gap (split) that serves as a capacitive element. However, the gap between the rings produces an inductive effect. The LC (inductive-capacitive) resonance produced by this combination is very sensitive to changes in the surrounding electromagnetic field [8, 9]. Microwave resonators, such as SRR, are important for the fabrication of small, high-sensitivity sensors [11]. SRR was first introduced as a metamaterial element with unique resonance properties owing to the combination of internal inductance and capacitance [14]. With the development of planar technology, the SRR structure was modified into a DSRR to enhance the electromagnetic interaction between the microwave field and the test material. Planar resonator-based sensors offer the advantages of compact sensor design, easy fabrication, and low cost [4].

According to previous research, sensors using the resonator method can detect material variations well. They created resonator-based sensors to measure the permittivity of solid and liquid materials. In previous studies, a resonator method was proposed to detect the permittivity of solid materials [5]. Subsequently, a DSRR was proposed to measure both solid and liquid permittivities [3, 8, 12]. The circular-split-ring resonator (CSRR) method has also been proposed to detect the permittivity of semi-solid materials [2, 16]. The results show that

* Corresponding author: Syah Alam (syah.alam@trisakti.ac.id).

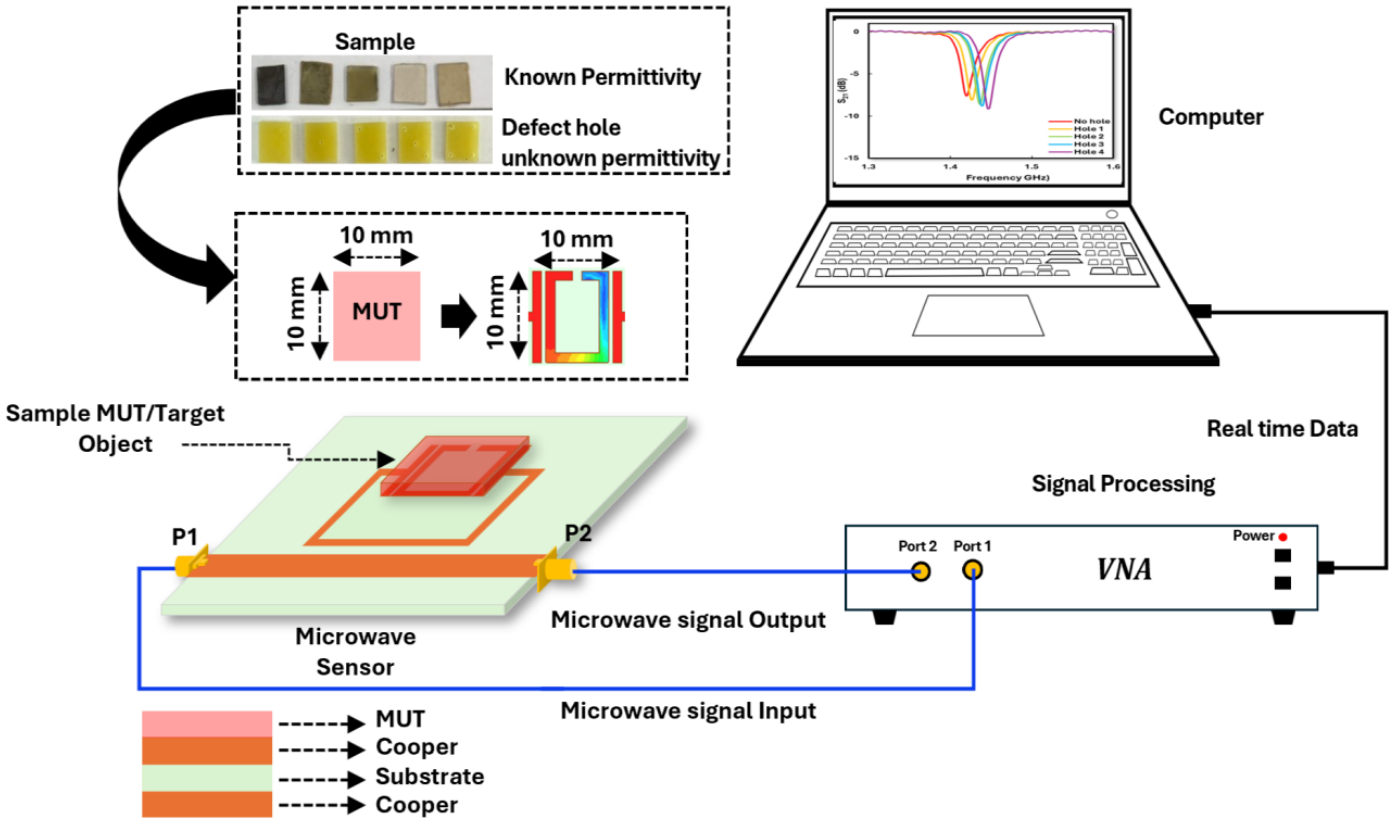


**FIGURE 1**. Proposed scenario microwave sensor for detecting material defects.

resonator-based sensors offer reliable and precise permittivity detection. The resonance frequency of the sensor indicates that the resonator method is highly sensitive to changes in the surrounding electromagnetic environment.

According to previous research, microwave sensors using the resonator method have been widely used to characterize the permittivity of solid or liquid materials but have not yet been used to detect the permittivity of defective materials. The detection of defective materials is necessary in the industry to ensure that the materials used are not damaged, thus disrupting the manufacturing process or the quality control of the resulting product. Therefore, a sensor capable of detecting the permittivity of defective materials is required. This study proposes a solution for producing a sensor capable of detecting the permittivity of defective materials. In this study, a hole with a fixed diameter of 1 mm was modeled. The holes were placed at several points according to the scenario proposed in this study. The addition of holes to represent defects in the material simulates physical defects that affect the electromagnetic field of the resonator. This resulted in changes in the resonant frequency (($fr$) and $S_{21}$ parameter. The resonator method using a dual-split-ring resonator (DSRR) can improve the quality factor of resonance and sensitivity to the permittivity of defective materials. The main contribution of this study is the design and implementation of a compact microwave sensor based on a dual-port architecture, that enables the characterization of solid samples and defects in materials.

## 2. WORKING PRINCIPLE OF MICROWAVE SENSOR FOR PERMITTIVITY DETECTION OF DEFECT MATERIAL

In this study, a microwave sensor is proposed to detect the permittivity of defects in materials using the resonance frequency shift approach and the change in transmission parameter $S_{21}$. The proposed microwave sensor is based on a dual-split-ring-resonator (DSRR) dual-port structure. Overall, the proposed sensor is shown in Figure 1. The sensor layout, experimental setup, and measurement flow are described in detail. The sensor was constructed on a resonance frequency of 1.5 GHz using a Rogers RO5880 substrate with a dielectric constant $\varepsilon_r$ of 2.2, tan $\delta$ of 0.0009, and a substrate thickness $h$ of 1.58.

The proposed microwave sensor employs a perturbation method as shown in Equation (1), which is used to characterize permittivity by observing resonance frequency shifts caused by placing a material under test (MUT) in the sensor area. This area has dimensions of 10 mm $\times$ 10 mm $\times$ 1 mm and was optimized to match the physical dimensions of the sample used in the experiment.

The process begins with the use of a reference sample with a known permittivity for the calibration process, followed by testing the MUT, which may have defects or unknown permittivity. The MUT with certain dimensions is placed above the sensitive area of the microstrip sensor, resulting in an interaction between the electromagnetic field and the material. The sensor was connected to a Vector Network Analyzer (VNA) via the input (P1)

and output (P2) ports, where a microwave signal is provided as the input, and the transmission response ($S_{21}$) is measured as the output. Changes in the field distribution due to the presence of the material and possible defects affect the effective permittivity, causing a shift in the resonance frequency that can be observed on a computer screen in real time. The obtained data are processed to determine the characteristics of the material, including the detection of defects. The sensor structure, which consists of a conductor layer (copper) and a dielectric substrate, allows for high sensitivity to changes in the electric field around the sensing area.

## 3. DESIGN AND SIMULATION

### 3.1. Development Model of Microwave Sensor

To maximize the performance of the proposed microwave sensor in detecting the permittivity of defective materials, three distinct sensor models were simulated. Each model was structurally modified to improve its resonance characteristics. The evolution of the microwave sensor models is shown in Figure 2(a), and beginning from the 1st step, the initial microwave sensor structure with dimensions $W = 50$ mm and $L = 50$ mm consists of a main transmission line connecting ports P1 and P2, combined with an open-loop resonator element placed above the main line. In this configuration, the electromagnetic coupling between the transmission line and resonator is still relatively weak. Subsequently, a second resonator was added to make the structure more complex and closer to the main line. This change strengthens the coupling effect, changes the resonant frequency, and changes the value of parameter $S_{21}$, which makes the system more sensitive. In the 2nd step, optimization was performed on the substrate length ($L$), with the substrate size reduced to 35 mm. In the 3rd step, optimization was performed on the gap parameter ($g_1$) between the feeding and resonator.

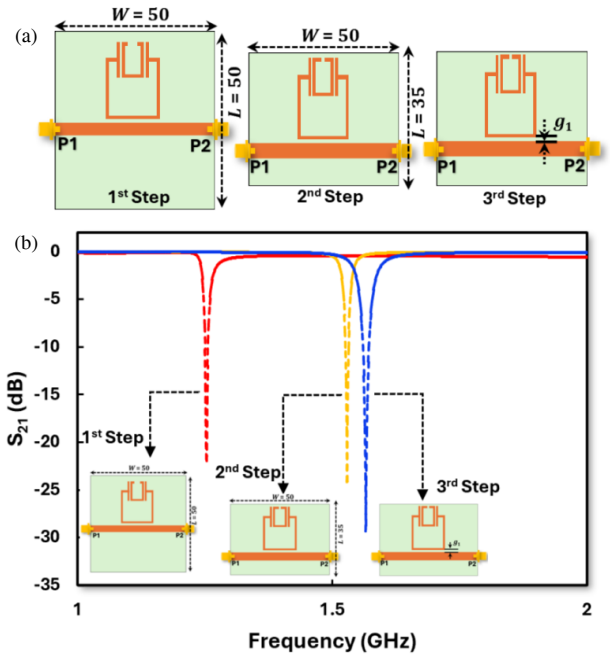


**FIGURE 2**. (a) SRR development model of 1st, 2nd, and 3rd steps and (b) Response $S_{21}$ at 1st, 2nd, and 3rd steps.

The simulated transmission coefficient ($S_{21}$) results are shown in Figure 2(b) and provide insight into the resonance behavior of each model. Model 1st step resonates at 1.253 GHz with a transmission coefficient ($S_{21}$) of $-22$ dB and has the lowest resonance frequency, indicating that the coupling is still limited. In the 2nd step, the model shows a higher resonance frequency and a deeper notch at 1.529 GHz with a transmission coefficient ($S_{21}$) of $-24.15$ dB, indicating that the coupling between the microstrip line and the resonator is still limited. In contrast, the sharpest and deepest notch is shown in the 3rd step, which indicates a resonance frequency of 1.566 GHz with a higher transmission coefficient of $-29.32$ dB.

### 3.2. Determination of the Location of the Sensing Area from the Proposed Microwave Sensor

The structural design and simulation results of the proposed microwave sensor are shown in Figure 3. As depicted in Figure 3(a), the graph shows that the transmission coefficient value $S_{21}$ is getting close to 0 dB. It means that the signal can be sent well (with low insertion loss). However, between 1.5 and 1.6 GHz, there is a sharp drop to about $-29.32$ dB. This means that the electromagnetic wave energy is not transmitted but instead absorbed by the resonator. This phenomenon suggests a band-stop (notch) filter, which significantly attenuates specific frequencies. The notch width is relatively small, which means that the structure has a high-quality factor (Q-factor). The structural configuration of the microwave sensor is shown in Figure 3(b), in which the overall dimensions of the microwave sensor and its structural parameters, such as length, width, and gap distance, are shown in the figure and explained in more detail in Table 1. The resonance frequency and substrate material quality dictate the size of the sensor antenna. The width ($W$) and length ($L$) of the microwave sensor patch were computed using the following equations [1, 2, 15]:

$$\frac{\Delta fr}{f_o} = \frac{\int_V (\Delta\varepsilon E_1 \cdot E_0 + \Delta\mu H_1 \cdot H_0)\, dv}{\int_v \left(\varepsilon_0 |E_0|^2 + \mu_0 \cdot |H_0|^2\right) dv} \tag{1}$$

**TABLE 1**. Dimension of the proposed microwave sensor.

| Parameters | Dimensions (mm) |
|---|---|
| $W$ | 50 |
| $L$ | 35 |
| $W_r$ | 17 |
| $L_r$ | 17 |
| $a_{1,2}$ | 1 |
| $b_{1,2}$ | 1 |
| $W_c$ | 7 |
| $L_c$ | 10 |
| $g_1$ | 0.4 |
| $g_2$ | 1 |
| $g_3$ | 0.5 |
| $L_z$ | 4 |

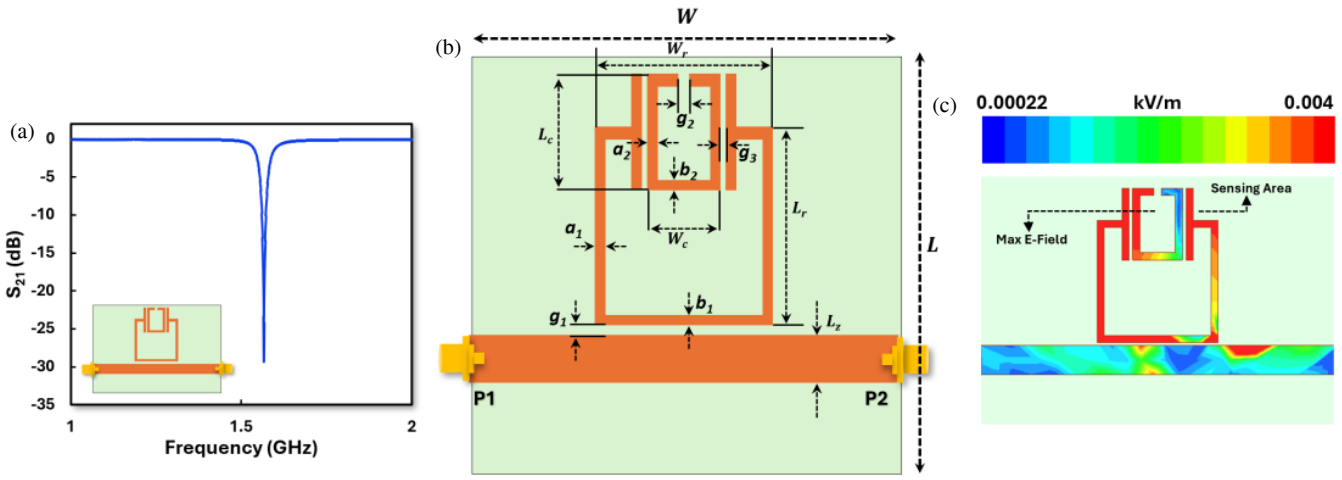


**FIGURE 3**. Simulation result and design of proposed microwave sensor; (a) simulated $S_{21}$, (b) structure of proposed DSRR microwave sensor, and (c) $E$-field concentration.

$$f_r = \frac{1}{2\pi\sqrt{LC}} \tag{2}$$

$$\lambda_g = \frac{C}{f\sqrt{\varepsilon_{eff}}} \tag{3}$$

$$\frac{W}{d} = \frac{8e^A}{e^{2A}-2} \tag{4}$$

$$A = \frac{Z_o}{60}\sqrt{\frac{\varepsilon_r+1}{2}}+\frac{\varepsilon_r-1}{\varepsilon_r+1}\left(0,23+\frac{0,11}{\varepsilon_r}\right) \tag{5}$$

$$\varepsilon_{eff} = \frac{\varepsilon_r+1}{2}+\frac{\varepsilon_r-1}{2}\left(\frac{1}{\sqrt{1+12\frac{h}{w}}}\right) \tag{6}$$

The first equation ($\Delta fr/f_o$) is a formulation of perturbation theory, which explains that changes in resonance frequency are due to changes in material properties ($\Delta\varepsilon$) and permeability ($\Delta\mu$), which interact with the distribution of the electric field ($E$) and magnetic field ($H$) within the sensor volume, thus forming the basis of the sensor's working principle in detecting materials. The equation ($f_r$) shows that the resonance frequency is determined by the equivalent inductance ($L$) and capacitance ($C$) of the resonator structure. Furthermore, ($\lambda_g$) describes the guided wavelength on the microstrip influenced by the effective dielectric constant. The ratio equation ($W/d$) and parameter ($A$) are used to determine the dimensions of the microstrip conductor width based on the characteristic impedance ($Z_o$) Ω, which is important for impedance matching in the proposed resonator. Finally, the equation ($\varepsilon_{eff}$) denotes the effective permittivity of the substrate at the given resonant frequency, and $h$ represents the thickness of the substrate (mm).

Figure 3(c) shows the distribution of the electric field ($E$-field) on the microwave sensor, expressed in kV/m, with a value range of approximately 0.00022 kV/m to 0.004 kV/m. The color map (color bar) shows that red indicates the highest electric field intensity, whereas blue indicates the lowest electric field intensity. This $E$-field distribution was obtained at the resonance frequency of the sensor, thus reflecting the optimal operating conditions of the resonator.

### 3.3. Simulation of Microwave Sensor for Detection of Permittivity and Hole Defect of MUT

Figure 4 shows a full simulation analysis of the proposed microwave sensor that was designed for microwave sensing applications, particularly for detecting permittivity in the range of 1 to 10. Using the High Frequency Structure Simulator (HFSS), tests were performed to determine how the frequency response of the proposed sensor changed when the dielectric properties of the materials being tested changed. As shown in Figure 4(a), the transmission coefficient ($S_{21}$) of the proposed sensor demonstrates a distinct resonance frequency shift as the relative permittivity ($\varepsilon_r$) increases, with the resonance frequency decreasing from 1.542 GHz at $\varepsilon_r = 1$ to 1.098 GHz at $\varepsilon_r = 10$. In the $S_{21}$ graph, it can be seen that the higher the permittivity of the material, the greater the shift of the resonance frequency to the left or to a lower frequency. This frequency shift indicates the sensitivity of the proposed sensor to changes in permittivity; therefore, small changes in the dielectric properties of the material can be observed through large shifts in the resonant frequency position. Thus, this graph shows that the sensor can characterize materials based on their permittivity differences.

To further quantify this behavior, Figure 4(b) introduces a polynomial fitting curve that models the relationship between resonance frequency and relative permittivity using the following equation:

$$f_r = 22.028\,(\varepsilon_r)^2 - 78.16\,(\varepsilon_r) + 69.197 \tag{7}$$

$f_r$ is the resonant frequency (GHz), and $\varepsilon_r$ is the relative permittivity. This equation reveals a significant correlation ($R^2 = 0.9998$), which confirms the accuracy of the sensor for measuring dielectric properties dependent on the frequency.

The sensitivity characteristics of the microwave sensor to changes in relative permittivity ($\Delta\varepsilon_r$) are shown by two main parameters, as shown in Figures 4(c) and Figure 4(d), frequency shift ($\Delta f$), and frequency detection resolution (FDR). In Fig-

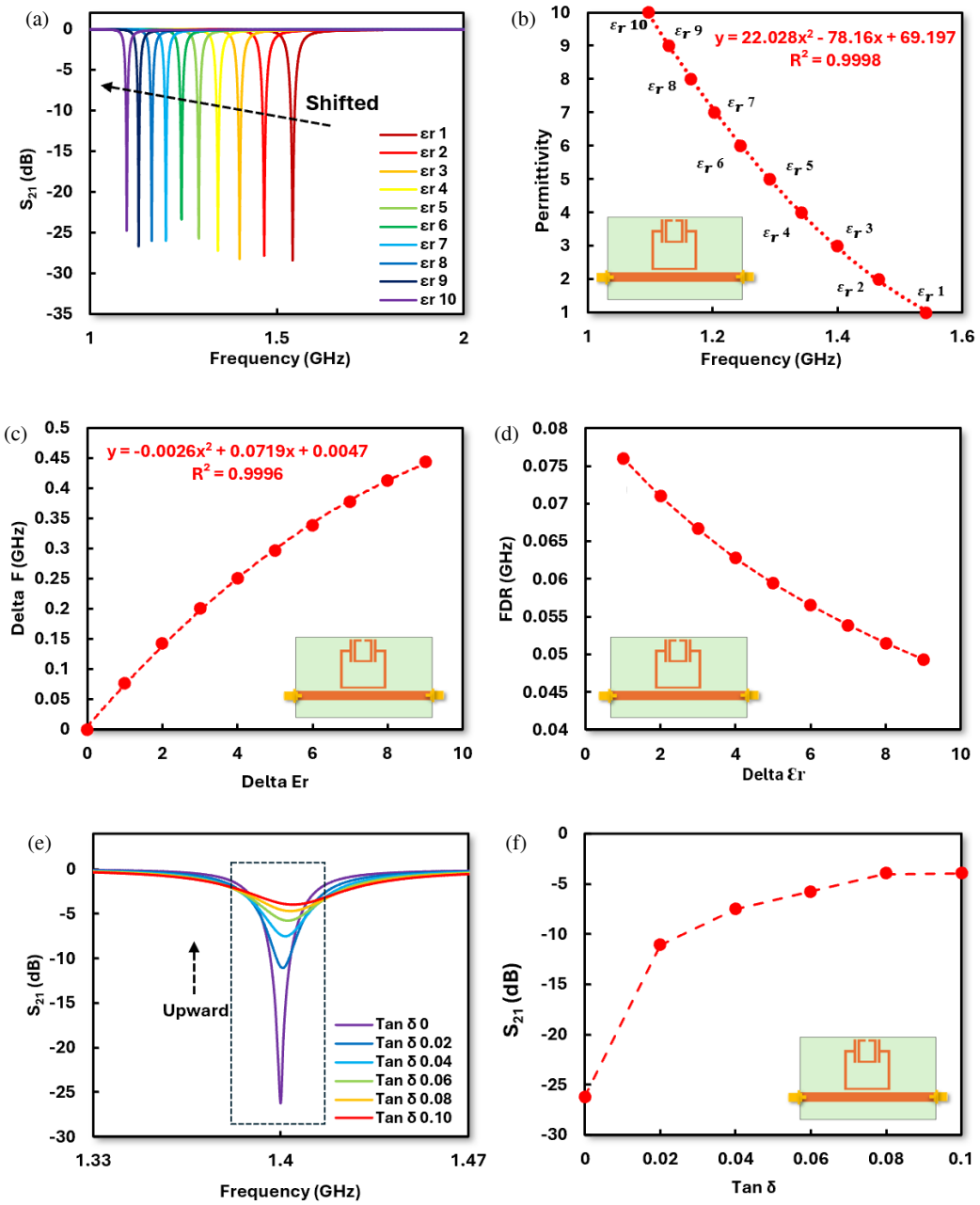


**FIGURE 4**. Simulation using proposed microwave sensor. (a) Correlation between frequency and permittivity. (b) Fitting curve for frequency detection. (c) $\Delta f$ of the proposed microwave sensor. (d) FDR of the proposed microwave sensor. (e) Simulation detection of tan delta with a range of 0–0.1. (f) Correlation between tan $\delta$ and $S_{21}$.

ure 4(c), it can be seen that $\Delta f$ increases nonlinearly with increasing $\Delta\varepsilon_r$, which is modeled by the polynomial equation.

$$\Delta f = -0.0026(\Delta\varepsilon_r)^2 + 0.0719(\Delta\varepsilon_r) + 0.0047 \quad (8)$$

with a very strong coefficient of determination ($R^2 = 0.9996$). This demonstrates the extremely excellent sensitivity of the sensor, where slight changes in the permittivity translate into large frequency shifts. The FDR value decreases with an increase in $\Delta\varepsilon_r$ as shown in Figure 4(d). This phenomenon shows a behaviour in the sensor response, especially in the higher permittivity region, where the increase in sensitivity is no longer proportional.

Figure 4(e) shows the resonance frequency response curve for tan $\delta$. Each increase in the tan $\delta$ value in the SUT causes the transmission coefficient to move lower or higher. The details are presented in Table 2.

Figure 4(f) shows the relationship between the loss tangent (tan $\delta$) and $S_{21}$ transmission parameter, which describes the effect of dielectric losses on the response of the resonance of microwave sensors. It is observed that the value of $S_{21}$ increased from $-26.23$ dB to $-3.96$ dB (less negative) with tan $\delta$ from 0 to 0.1. This implies that the higher the value of tan $\delta$, the higher the dielectric loss in the material. The resonance is significantly weaker, as shown by the reduction in the depth of the notch in

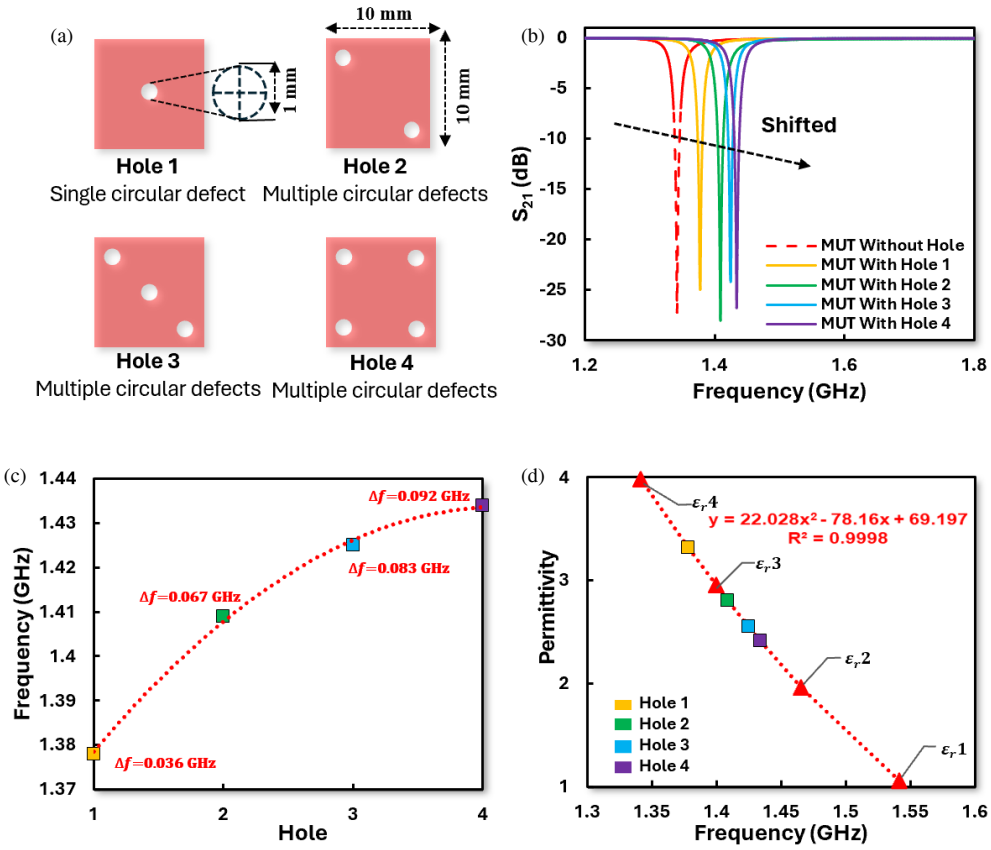


**FIGURE 5**. Simulation using proposed microwave sensor, (a) MUT hole models, (b) response $S_{21}$ is defective in MUT, (c) $\Delta f$ of proposed hole defect, and (d) correlation $f_r$ and permittivity hole.

**TABLE 2**. $S_{21}$ values from the simulation results of dielectric tan $\delta$ MUT.

| Tan $\delta$ | $S_{21}$ (dB) |
|---|---|
| 0 | −26.23 |
| 0.02 | −11.08 |
| 0.04 | −7.54 |
| 0.06 | −5.78 |
| 0.08 | −3.97 |
| 0.1 | −3.96 |

the $S_{21}$ curve. At small tan $\delta$ values, the resonance appears very sharp and deep (deep notch), indicating a high-quality factor (Q-factor). In contrast, at a large loss tangent (tan $\delta$), the curve becomes shallower, indicating the decrease of the Q-factor and weakening of the structural ability to retain the resonance energy. Therefore, this graph shows that the $S_{21}$ parameter is very sensitive to the change of loss tangent (tan $\delta$).

This Material Under Test (MUT) was modelled to have artificial defects in the form of circular holes to represent defects in the material, as shown in Figure 5(a). Variations in the number and distribution of holes are used to simulate the level of material inhomogeneity, whereas the circular shape of the holes was chosen because it is electromagnetically stable, easy to model, and capable of representing nonhomogeneous material defects while minimizing the $E$-field concentration at sharp corners. The addition of holes to the MUT theoretically affects the microwave sensor response because part of the material volume with high relative permittivity is replaced by air with low permittivity. This condition causes a decrease in the effective permittivity of the material $\varepsilon_{eff}$ that directly interacts with the resonator's electric field.

Figure 5(b) shows the transmission parameter $S_{21}$ characteristics of the resonator-based microwave sensor when the MUT is given an additional variation in the number of holes. The reference curve without holes (MUT) shows resonance at the lowest frequency, indicating that the intact material structure has the highest effective permittivity. Under the condition of a hole-free MUT, the resonance frequency is at a specific position. When a hole is added to the MUT, the material structure becomes nonhomogeneous, resulting in a change in the electric field distribution around the resonator. The holes in the MUT generally contain air ($\varepsilon_r = 1$), thereby reducing the overall effective permittivity of the material compared to the intact MUT. When a hole is added, the value of $\varepsilon_{eff}$ decreases, causing the equivalent capacitance of the resonator to also decrease. Consequently, the resonance frequency shifts to a higher direction (right shift).

Figure 5(c) continues this analysis by illustrating the absolute frequency shift ($\Delta f$) in response to a change in permittivity ($\Delta \varepsilon_r$) across a material defect [6]:

$$\Delta f(\%) = \frac{f - f_o}{f_o} \times 100\% \tag{9}$$

**TABLE 3**. Correlation of $f_r$ and hole in MUT.

| Number of holes | Frequency (GHz) | $\Delta f$ | |
|---|---|---|---|
| | | (GHz) | % |
| 1 | 1.378 | 0.036 | 2.68 |
| 2 | 1.409 | 0.067 | 5 |
| 3 | 1.425 | 0.083 | 6.18 |
| 4 | 1.434 | 0.092 | 6.86 |

$\Delta f$ stands for the frequency shift (GHz), $f_o$ the initial resonance frequency, and $f$ the frequency after the change.

Table 3 quantitatively shows the correlation between resonance frequency and number of holes of SUT. Based on the simulation results, increasing the number of holes from 1 to 4 causes an increase in the resonance frequency from 1.378 GHz to 1.434 GHz. The frequency shift value ($\Delta f$) also increases from 0.036 GHz to 0.092 GHz; the increase in $\Delta f$ hole 1 is 2.68%; that in $\Delta f$ hole 2 is 5%; that in $\Delta f$ hole 3 is 6.18%; and that in $\Delta f$ hole 4 is 6.86%, which shows that the structure becomes more sensitive to changes (Figure 5(d)). The visible pattern shows that the higher the permittivity of a material, the lower the resonance frequency produced by the DSRR structure.

## 4. MEASUREMENT AND VALIDATION

### 4.1. Measurement Process and Validation with Known Permittivity

In this study, the proposed sensor was fabricated using RO5880 with a permittivity of 2.2, $\tan\delta$ of 0.0009, and a thickness of 1.58 mm. Rogers RO5880 was selected because it exhibits a very low moisture absorption rate (approximately 0.02%), which helps maintain stable dielectric properties under normal laboratory conditions. In this work, all measurements were conducted in a controlled indoor environment with relatively constant temperature and humidity to minimize environmental effects. To ensure uniform electrical properties, the substrate used in the fabrication was obtained directly from the manufacturer with specified dielectric constant and thickness tolerances based on the datasheet. Before fabrication and measurement, the Rogers RO5880 substrate was carefully inspected visually to ensure that no visible cracks, scratches, or mechanical defects were present on the substrate surface. The substrate thickness ($h = 1.58$ mm) was measured using a precision caliper/micrometer at multiple locations to verify thickness consistency.

Experimental validation of the proposed microwave sensor's capabilities can be seen in Figure 6. Figure 6(a) shows the physical setup used to perform permittivity detection using the fabricated microwave sensor. The sensor is connected to a vector network analyzer (VNA) through ports 1 and 2 as the output signal to measure the transmission coefficient $S_{21}$. The microwave sensor is mounted on a standard printed circuit board (PCB) substrate, and various test materials are placed on the sensing area. These materials include dielectric materials such as RO-5880, RO-4003, RO-3006, FR-4, and TM-10, as well as MUT samples whose permittivity is not known to be a material defect. A frequency sweep step of 0.002 GHz was used. All samples have identical dimensions of $10 \times 10$ mm and identical thickness.

To evaluate the accuracy of the fabricated sensor, a comparison between the simulated and measured $S_{21}$ is presented in Figure 6(b). In the simulation, the resonance frequency is 1.56 GHz with an $S_{21}$ value of $-29.01$ dB, while the measurement results show a slightly higher frequency of 1.61 GHz and an $S_{21}$ of $-11.4$ dB. To assess the performance of the fabricated sensor and identify any deviations from the simulated behavior, an error analysis is performed by comparing the resonance frequencies obtained from both simulation and measurement using the following equation:

$$\text{Error}\,(\%) = \frac{f_{measured} - f_{simulated}}{f_{simulated}} \times 100\% \tag{10}$$

The error result indicates a deviation of approximately 3.21%, which is rather little and remains within acceptable parameters for practical sensor use. Differences between simulation and measurement results are generally driven by several interrelated technical factors. Physically, fabrication tolerances, such as inaccuracies in the copper etching process and variations in substrate thickness, can alter the dimensions of the microstrip channel, directly shifting the impedance and resonant frequency. Simulations typically use nominal permittivity values (typically $\varepsilon_r = 2.2$), and the RO5880 permittivity can vary from 2.18 to 2.22. Small changes in this ($\varepsilon_r$) can have a measurable impact on the sensor's resonant behavior. Furthermore, the anisotropy and roughness of the copper surface increase losses in real devices. On the other hand, model mismatches often arise from interconnection and environmental factors. The use of SMA connectors and the soldering process often introduce parasitic capacitances that are not perfectly modeled in ideal simulations. Finally, the accuracy of measurement results also depends heavily on the precision of the VNA instrument calibration and the influence of objects around the sensor that can interfere with the fringing field.

Based on these validation results, Figure 6(c) shows the $S_{21}$ sensor's response to six different dielectric materials with known permittivity values. The specifications for the six dielectric materials and their $S_{21}$ responses are listed in Table 4,

The ($S_{21}$) frequency response graphs for permittivity changes show a clear frequency shift for various materials, such as air or vacuum, RO5880, RO4003C, FR4, RO3006, and TM10. As the permittivity value increases from 1 to 9.8, the

**TABLE 4**. $S_{21}$ parameter with known permittivity.

| Materials | Permittivity | Frequency (GHz) | $S_{21}$ (dB) |
|---|---|---|---|
| Vacuum/Air | 1 | 1.61 | −11.713 |
| Rogers RT/duroid 5880 | 2.2 | 1.574 | −12.06 |
| Rogers RO4003C | 3.55 | 1.548 | −12.73 |
| FR4 | 4.3 | 1.51 | −9.42 |
| Rogers RO3006 | 6.15 | 1.448 | −12.73 |
| Rogers TM10i | 9.8 | 1.242 | −6.76 |

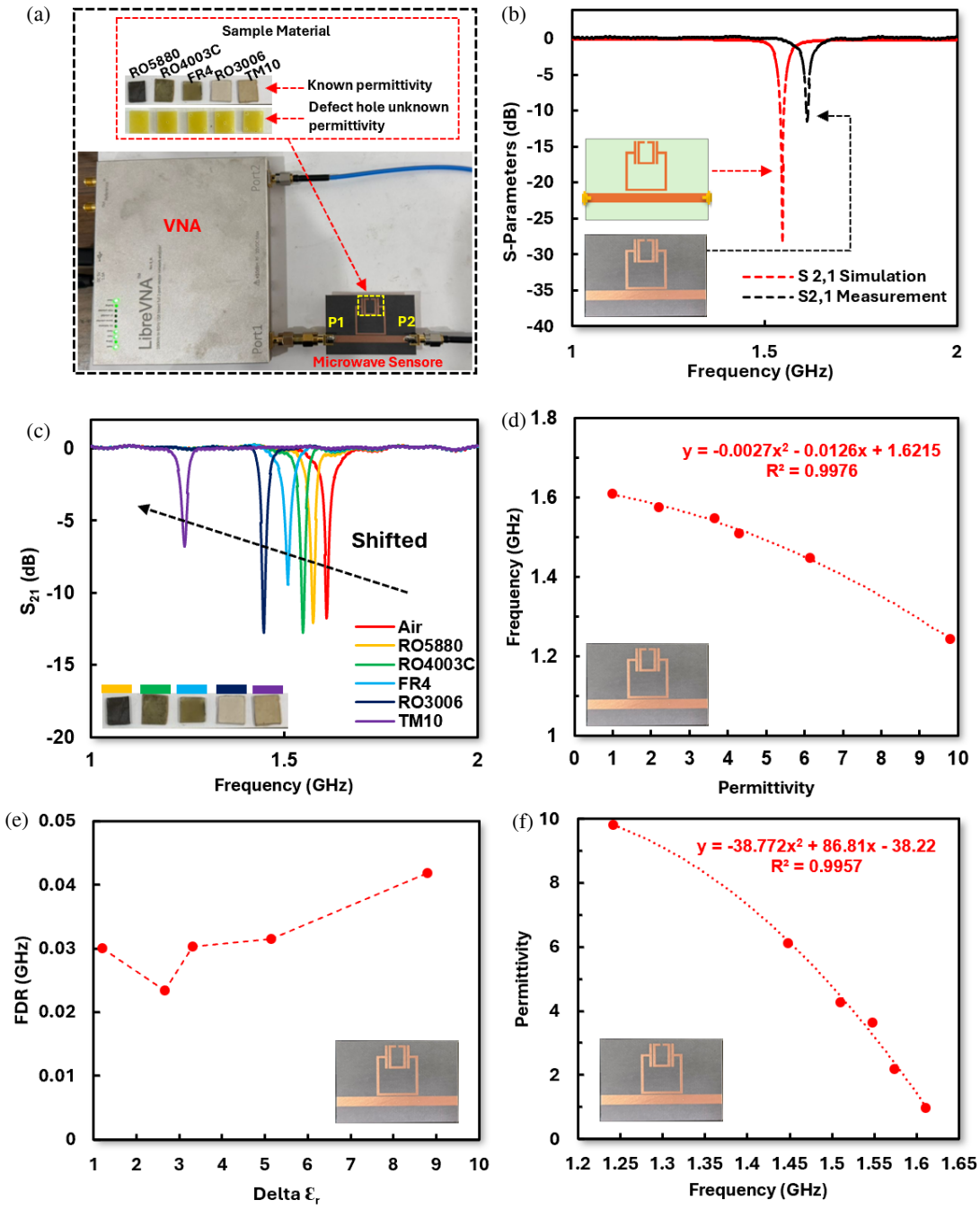


**FIGURE 6**. Measurement of the proposed DSRR microwave sensor for known permittivity materials. (a) Setup for detection using microwave sensor, (b) $S_{21}$ simulation and measurement result, (c) response of frequency with permittivity changes, (d) fitting curve for permittivity detection, (e) FDR for permittivity detection, and (f) fitting curve for permittivity detection.

resonance frequency decreases significantly from 1.61 GHz to 1.242 GHz. This is in accordance with the principle that the resonance frequency is inversely proportional to the square root of the effective permittivity, so the larger the $\varepsilon_r$, the lower the resonance frequency. In addition, the $S_{21}$ value indicates the variation in resonance depth, where most materials, such as Rogers RO4003C and RO3006, produce a deeper notch (around $-12.73$ dB), indicating strong resonance and good coupling. In contrast, materials with very high permittivity, such as Rogers TMM10i, exhibit a shallower $S_{21}$ value ($-6.76$ dB), indicating reduced resonance quality.

The graph shows the relationship between permittivity ($\varepsilon_r$) and resonance frequency, which follows a nonlinear decreasing trend as shown in Figure 6(d). As the permittivity value increases from about 1 to 10, the resonance frequency drops from about 1.61 GHz to 1.24 GHz. This relationship is modelled by the polynomial model as shown in the following equation:

$$f_r = -0.0027\,(\varepsilon_r)^2 - 0.0126\,(\varepsilon_r) + 1.6215 \qquad (11)$$

with a coefficient of determination value of $R^2 = 0.9976$, which shows a very high level of fit between the model and the data. It indicates that changes in permittivity have a significant and measurable effect on the resonance frequency. The nonlinear curve shows that the sensor exhibits nonuniform sensitivity across the measurement range, where at higher permittivity values, the frequency decrease becomes more significant. The graph in Figure 6(e) shows the relationship between the permittivity change ($\Delta\varepsilon_r$) and the frequency detection resolution (FDR), which represents the sensor's sensitivity to material variations. In general, it can be seen that the FDR value tends to increase with increasing $\Delta\varepsilon_r$, although there is a slight decrease in the $\Delta\varepsilon_r$ value before gradually increasing again to reach the maximum value of around 0.042 GHz at the highest $\Delta\varepsilon_r$. This trend indicates that the greater the permittivity difference in the material, the greater the resulting frequency shift, which means that the sensor's sensitivity increases. However, the presence of small fluctuations at the beginning of the curve indicates that the sensor's response is not completely linear, possibly influenced by the electromagnetic field distribution or coupling effects in the structure. Figure 6(f) displays a polynomial fitting curve of the relationship between permittivity and resonant frequency based on measured data of known permittivity as shown in the following equation:

$$\varepsilon_r = -38.772\,(f_r)^2 + 86.81\,(f_r) - 38.22 \tag{12}$$

with a high coefficient of determination value $R^2 = 0.9957$), which shows that the model has very good accuracy in representing the data.

To validate the accuracy of the proposed sensor in detecting materials with known permittivity, a series of measurements was conducted using reference dielectric samples, such as air or vacuum, RO5880, RO4003C, FR4, RO3006, and TM10. The results show high consistency between the measured and reference permittivity values, thus confirming the reliability and precision of the sensor. Sensor accuracy when materials are used with the measured permittivity is shown in Table 5.

**TABLE 5**. Comparative measurements of microwave sensors for materials with known permittivity.

| Materials | Permittivity | Error (%) | Accuracy (%) |
|---|---|---|---|
| Vacuum/Air | 1 | 0.24 | 99.76 |
| Rogers RT/duroid 5880 | 2.2 | 0.43 | 99.57 |
| Rogers RO4003C | 3.55 | 0.55 | 99.45 |
| FR4 | 4.3 | 0.49 | 99.51 |
| Rogers RO3006 | 6.15 | 0.42 | 99.57 |
| Rogers TM10i | 9.8 | 0.26 | 99.73 |

The minimum error observed in air or vacuum was only 0.24%, resulting in a near-perfect accuracy of 99.76%. The average error was 0.4%, and the average accuracy was 99.6%. All samples were above 99%, confirming the sensor's effectiveness in detecting subtle changes in dielectric properties.

To further evaluate the accuracy of the sensor and the sensor's response to changes in the dielectric constant, important performance parameters were determined from the microwave sensor's frequency response to known permittivity materials. These metrics are absolute frequency shift ($\Delta f$), normalized sensitivity (NS), and frequency detection resolution (FDR) that evaluate the sensor's sensitivity, accuracy, and ability to detect small changes in permittivity together. The following equations provide further insight into the operational effectiveness of the sensor and how these parameters are derived [7].

$$NS = \frac{1}{\varepsilon_r} x \left( \frac{f_{unloaded} - f_{loaded}}{f_{unloaded}} \right) \% \tag{13}$$

Normalized Sensitivity (NS), which measures how responsive a sensor is to changes in the dielectric properties of the material being tested relative to its own resonant frequency. In other words, NS measures the normalized sensitivity of a sensor, so the results are independent of the sensor's operating frequency [7].

$$FDR = \frac{\Delta f}{\Delta \varepsilon_r} (GHz) \tag{14}$$

FDR is calculated based on the magnitude of the change in the sensor's resonance frequency when a material with a certain dielectric constant is placed in the sensing area. Mathematically, FDR is expressed as the ratio of the change in resonance frequency to the change in dielectric constant.

### 4.2. The Process of Measuring and Validating Defective Materials with Unknown Permittivity

The proposed microwave sensor was measured and validated using a MUT sample with unknown permittivity material, as shown in Figure 7; the measured sample was configured with the addition of circular holes as a representation of defects in the material. Figure 7(a) shows the $S_{21}$ transmission response; the notch position shifts towards higher frequencies (shifted to the right) as the number of holes increases from the condition without holes to four holes. This shift indicates that the presence of holes causes a decrease in the effective permittivity ($\varepsilon_{eff}$) due to the presence of air cavities ($\varepsilon \approx 1$), so that electromagnetic waves propagate faster, and the resonance frequency increases. With more holes, the electric field distribution in the sensing area becomes more disturbed and concentrated, thereby increasing the sensor's sensitivity to changes in material structure. Thus, the number of hole defects has a significant influence on resonance characteristics and can be used as a parameter to detect and characterize defects in materials nondestructively.

**TABLE 6**. Frequency shift of MUT with hole configuration.

| Hole | Freuency (GHz) | Predict $\varepsilon_r$ |
|---|---|---|
| No Hole | 1.42 | 6.8703392 |
| Hole 1 | 1.426 | 6.729128528 |
| Hole 2 | 1.436 | 6.487573888 |
| Hole 3 | 1.44 | 6.3887808 |
| Hole 4 | 1.446 | 6.238264848 |

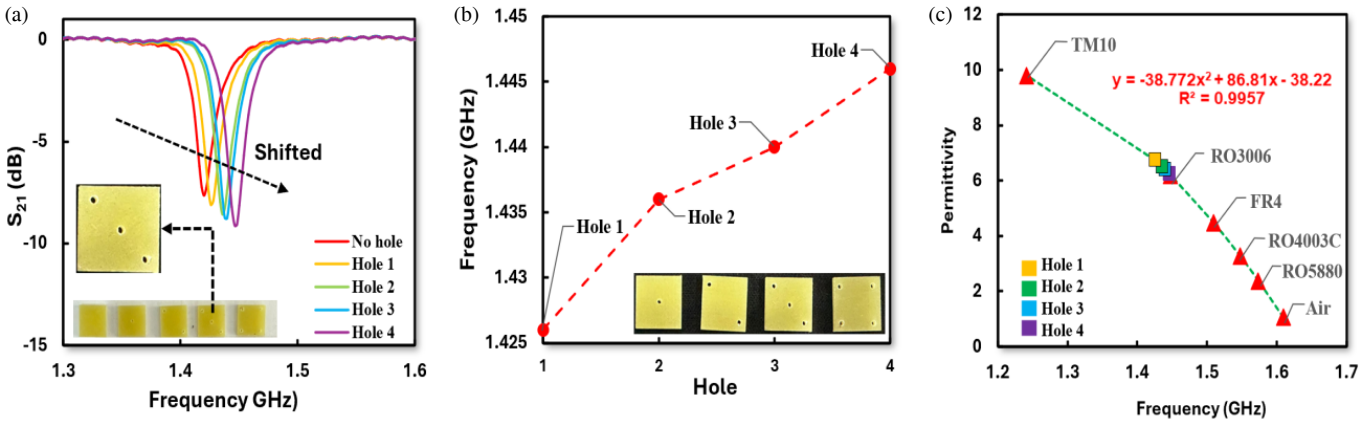


**FIGURE 7**. Measurement of the proposed DSRR microwave sensor for unknown permittivity materials. (a) $S_{21}$ frequency response to material defects, (b) correlation between tan $\delta$ and $S_{21}$, and (c) Correlation $f_r$ and permittivity.

**TABLE 7**. Comparison of the proposed microwave sensor with existing works.

| Ref | Method | $f_r$ (GHz) | Permittivity Range | Samples | Port Configuration | Sensing Performance | | | Capability for defect material |
|---|---|---|---|---|---|---|---|---|---|
| | | | | | | FDR | Acc. (%) | NS (%) | |
| [5] | Antenna with U-Slot | 2.53 | 1–4.3 | Solid | Single | 0.012 | 96 | 0.0015 | No |
| [3] | DSRR | 2.27 | 1–4.3 | Solid | Dual | 0.29 | 85 | 0.039 | No |
| [8] | DSRR | 2.45 | 1–5.65 | Solid Liquid | Dual | NA | NA | 2.58 0.30 | No |
| [2] | Triple ring CSRR | 2.5 | 1–78.4 | Semi solid | Dual | NA | NA | 4.806 | No |
| [16] | CSRR | 3.37 | 1–4.3 | Solid | Dual | 0.47 | 87 | 0.042 | No |
| This work | DSRR | 1.5 | 1–9.8 | Solid Defect Material | Dual | 0.026 | 99.6 | 2.6 | Yes |

The relationship between the number of holes (defects) in the MUT and the resonant frequency is shown in Figure 7(b). It can be seen that the frequency increases gradually from 1.426 GHz at 1 hole to 1.446 GHz at 4 holes. This trend indicates that increasing the number of holes causes a shift in the frequency towards a higher direction. This phenomenon occurs because the presence of holes reduces the effective permittivity ($\varepsilon_{eff}$) of the material, because air has a much lower permittivity than solid materials. In addition, the increase in frequency, which tends to be nonlinear, indicates a saturation effect or the limited influence of additional holes on the distribution of the electromagnetic field.

The relationship between permittivity ($\varepsilon_r$) and resonance frequency for variations in the number of holes (Hole 1 to Hole 4) shows a decreasing nonlinear trend as in Figure 7(c). This relationship is modeled by a polynomial equation, as in the equation $12\varepsilon_r = -38.772\,(f_r)^2 + 86.81\,(f_r) - 38.22$, with a very high coefficient of determination value ($R^2 = 0.9957$), which indicates that the model fits the experimental data very well. This phenomenon is physically in line with the principle that the resonance frequency is inversely proportional to the effective permittivity, which means that materials with high permittivity produce lower frequencies, while the addition of holes (which indicate air cavities with low permittivity) will increase the resonance frequency. The corresponding data for frequency shifts is summarized in Table 6.

The data presented in Table 6 shows a correlation between the physical structure of the material and its electromagnetic properties. With an increasing number of holes, the frequency value gradually increases from 1.42 GHz to 1.446 GHz with 4 holes. On the other hand, the predicted $\varepsilon_r$ constant value consistently decreases, from 6.870 to 6.238. This phenomenon occurs because the addition of holes (air) into a solid material structure reduces the material's density, which technically lowers its effective permittivity.

## 5. COMPARISON WITH PREVIOUS WORK

To validate this work, the performance of the proposed microwave sensor is compared with existing microwave sensors in

the previous literature, as shown in Table 7. The compared sensor performance includes several parameters such as resonance frequency, sample type, permittivity range, accuracy, sensitivity, and the ability to detect the permittivity of defective materials.

The previous sensor by [5] utilized a U-slot antenna structure operating at 2.53 GHz, achieving a frequency detection resolution (FDR) of 0.012 and an accuracy of 96% for permittivities ranging from 1 to 4.13, though its normalized sensitivity (NS) was low at 0.0015. In contrast, dual-port designs like the dual-split-ring resonator (SRR) [3] and nested CSRR [16] exhibited wider FDR values of 0.29 and 0.47, respectively, with lower accuracy (85% and 87%) and higher NS values (0.039 and 0.042), indicating less precision in permittivity estimation. A two-ring asymmetric rectangular DSRR [8] at 2.45 GHz measured solids and liquids from 1 to 5.65 with NS values of 2.58% and 0.30%. The nested CSRR also showed lower accuracy and higher NS values. A triple-ring dual-port CSRR model [2] at 2.5 GHz effectively detects permittivity in semi-solid materials, achieving an NS of 4.806%, although its FDR and average accuracy remain unspecified, suggesting that more resonator structures enhance sensor performance.

Finally, the DSRR-based microwave sensor with a working frequency of 1.5 GHz is capable of covering a wider range of permittivity (1–9.8) and is applied not only to solid materials but also for detecting the permittivity of defective materials. The proposed sensor using a dual-port configuration shows excellent performance with an accuracy of 99.6% and an NS value of 2.6%, which is much higher than most previous studies. Although the FDR value (0.026) is not as high as in some other studies, the combination of high accuracy, good sensitivity, and defect detection capability makes the proposed design superior and more comprehensive.

## 6. CONCLUSION

From the obtained parameters, it can be concluded that the designed microwave sensor has excellent performance in material characterization. The sensor operates at the frequency of 1.5 GHz with a dual-port configuration to obtain accurate transmission measurements. The wide permittivity range (1–9.8) demonstrates the ability of the sensor to identify different types of materials, both solid and materials that have defects. The FDR value of 0.026 indicates that there is a stable frequency response. A very high accuracy (99.6%) confirmed that the measurement results were reliable. Moreover, the normalized sensitivity (NS) value of 2.6% indicates that the sensor has good sensitivity towards permittivity changes. Overall, these parameters demonstrate that this sensor is effective, accurate, and has great potential for nondestructive material characterization and defect detection applications.

Although the proposed sensor has advantages in terms of high accuracy, good sensitivity, and defect detection capability, there are still limitations in terms of FDR value, frequency flexibility, and response nonlinearity. With further development in structural design and sensitivity improvement, it will become a more sophisticated, adaptive, and applicable material characterization system in the future.

## REFERENCES


[1] Al-behadili, A. A., T. Petrescu, and I. A. Mocanu, "Complimentary split ring resonator sensor with high sensitivity based on material characterization," *TELKOMNIKA (Telecommunication Computing Electronics and Control)*, Vol. 18, No. 1, 272–281, 2020.

[2] Al-Gburi, A. J. A., N. A. Rahman, Z. Zakaria, and M. Palandoken, "Detection of semi-solid materials utilizing triple-rings CSRR microwave sensor," *Sensors*, Vol. 23, No. 6, 3058, 2023.

[3] Al-Gburi, A. J. A., Z. Zakaria, I. M. Ibrahim, R. S. Aswir, and S. Alam, "Solid characterization utilizing planar microwave resonator sensor," *Applied Computational Electromagnetics Society Journal (ACES)*, Vol. 37, No. 2, 222–228, 2022.

[4] Alahnomi, R. A., Z. Zakaria, Z. M. Yussof, A. A. Althuwayb, A. Alhegazi, H. Alsariera, and N. A. Rahman, "Review of recent microwave planar resonator-based sensors: Techniques of complex permittivity extraction, applications, open challenges and future research directions," *Sensors*, Vol. 21, No. 7, 2267, 2021.

[5] Alam, S., I. Surjati, R. D. Mardian, L. Sari, G. Daffin, Iznih, Z. Zakaria, L. D. Asrar, and T. Firmansyah, "Close quarters permittivity detection based on tagging antenna sensor for solid material characterization," *Progress In Electromagnetics Research C*, Vol. 154, 21–29, 2025.

[6] Alibakhshikenari, M., B. S. Virdee, T. A. Elwi, I. D. Lubangakene, R. K. R. Jayanthi, A. A. Al-Behadili, Z. A. A. Hassain, S. M. Ali, G. Pau, P. Livreri, and S. Aïssa, "Design of a planar sensor based on split-ring resonators for non-invasive permittivity measurement," *Sensors*, Vol. 23, No. 11, 5306, 2023.

[7] Anggradinata, H. N. and M. Asvial, "Multifunctional dual-band microwave sensor for the detection of liquid permittivity and solid displacement," *Progress In Electromagnetics Research C*, Vol. 152, 131–141, 2025.

[8] Jang, S.-Y. and J.-R. Yang, "Double split-ring resonator for dielectric constant measurement of solids and liquids," *Journal of Electromagnetic Engineering and Science*, Vol. 22, No. 2, 122–128, 2022.

[9] Kim, B.-H., Y.-J. Lee, H.-J. Lee, Y. Hong, J.-G. Yook, M. H. Chung, W. Cho, and H. H. Choi, "A gas sensor using double split-ring resonator coated with conducting polymer at microwave frequncies," in *SENSORS, 2014 IEEE*, 1815–1818, Valencia, Spain, 2014.

[10] Krupka, J., "Microwave measurements of electromagnetic properties of materials," *Materials*, Vol. 14, No. 17, 5097, 2021.

[11] Leibl, N., K. Haupt, C. Gonzato, and L. Duma, "Molecularly imprinted polymers for chemical sensing: A tutorial review," *Chemosensors*, Vol. 9, No. 6, 123, 2021.

[12] Masrakin, K., S. Z. Ibrahim, H. A. Rahim, S. N. Azemi, P. J. Soh, and S. Tantiviwat, "Microstrip sensor based on ring resonator coupled with double square split ring resonator for solid material permittivity characterization," *Micromachines*, Vol. 14, No. 4, 790, 2023.

[13] Muñoz-Enano, J., P. Vélez, M. Gil, and F. Martín, "Planar microwave resonant sensors: A review and recent developments," *Applied Sciences*, Vol. 10, No. 7, 2615, 2020.

[14] Pendry, J. B., A. J. Holden, D. J. Robbins, and W. J. Stewart, "Magnetism from conductors and enhanced nonlinear phenomena," *IEEE Transactions on Microwave Theory and Techniques*, Vol. 47, No. 11, 2075–2084, 1999.

[15] Pozar, D., *Microwave Engineering*, Springer, 2018.

[16] Abd Rahman, N., Z. Zakaria, R. A. Rahim, M. A. M. Said, A. A. M. Bahar, R. A. Alahnomi, and A. Alhegazi, "High quality factor using nested complementary split ring resonator for dielec-

tric properties of solids sample," *Applied Computational Electromagnetics Society Journal (ACES)*, Vol. 35, No. 10, 1222–1227, 2020.

[17] Soffiatti, A., Y. Max, S. G. Silva, and L. M. d. Mendonça, "Microwave metamaterial-based sensor for dielectric characterization of liquids," *Sensors*, Vol. 18, No. 5, 1513, 2018.

[18] Haq, T. U., C. Ruan, X. Zhang, and S. Ullah, "Complementary metamaterial sensor for nondestructive evaluation of dielectric substrates," *Sensors*, Vol. 19, No. 9, 2100, 2019.